

# Microdialysis in the Rat Striatum: Effects of 24 h Dexamethasone Retrodialysis on Evoked Dopamine Release and Penetration Injury

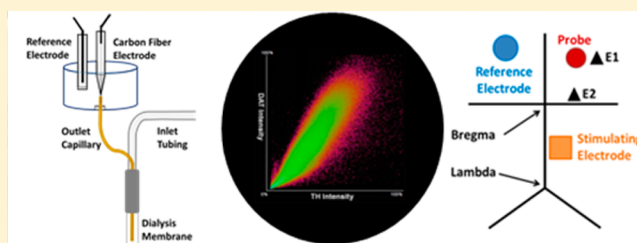
Kathryn M. Nesbitt, Erika L. Varner, Andrea Jaquins-Gerstl, and Adrian C. Michael\*

Department of Chemistry, University of Pittsburgh, Pittsburgh, Pennsylvania 15260, United States

## Supporting Information

**ABSTRACT:** The power of microdialysis for in vivo neurochemical monitoring is a result of intense efforts to enhance microdialysis procedures, the probes themselves, and the analytical systems used for the analysis of dialysate samples. Our goal is to refine microdialysis further by focusing attention on what happens when the probes are implanted into brain tissue. It is broadly acknowledged that some tissue damage occurs, such that the tissue nearest the probes is disrupted from its normal state. We hypothesize that mitigating such disruption would refine microdialysis. Herein, we show that the addition of dexamethasone, an anti-inflammatory drug, to the perfusion fluid protects evoked dopamine responses as measured by fast-scan cyclic voltammetry next to the probes after 24 h. We also show that dexamethasone stabilizes evoked dopamine responses measured at the probe outlet over a 4–24 h postimplantation interval. The effects of dexamethasone are attributable to its anti-inflammatory actions, as dexamethasone had no significant effect on two histochemical markers for dopamine terminals, tyrosine hydroxylase and the dopamine transporter. Using histochemical assays, we confirmed that the actions of dexamethasone are tightly confined to the immediate, local vicinity of the probe.

**KEYWORDS:** Microdialysis, voltammetry, dopamine, dexamethasone, immunohistochemistry, penetration injury



Intracranial microdialysis has made multiple seminal contributions to our knowledge of the neurochemistry of the living brain.<sup>1–14</sup> The benefits and power of microdialysis for intracranial chemical monitoring, which are well-known and have been reviewed often,<sup>15–23</sup> stem from the efforts of many laboratories to refine both the microdialysis probes and the instrumental methods used to analyze dialysate samples.<sup>24–29</sup> There has been tremendous progress, for example, in lowering the detection limits for key substances, including neurotransmitters, which has in turn reduced sampling times and increased temporal resolution.<sup>30–34</sup> Here, we wish to contribute to this ongoing refinement effort by focusing attention on what happens when the probes are implanted into brain tissue.

Typical microdialysis probes, those in widespread use, have diameters of at least 250  $\mu\text{m}$ .<sup>23,35–37</sup> Implanting these into the brain causes tissue damage, which in turn triggers a wound response.<sup>38–50</sup> The wound response involves a cascade of events, some of which begin right away and some of which develop over the course of several days. Microglial cells respond within minutes to focal brain injury, whereas astrocytes respond later.<sup>51,52</sup> Astrocytes form a scar around microdialysis probe tracks by 5 days postimplantation.<sup>41</sup> Probe implantation also causes ischemia, disruption of the blood-brain barrier, and neuron loss.<sup>40–43</sup> Neurochemical instability over the post-implantation intervals has been reported as well.<sup>35,37,53–58</sup> Even so, the dialysate content of neurotransmitters exhibits sensitivity to tetrodotoxin,<sup>2</sup> responds predictably to various drugs,<sup>28,59–61</sup> and correlates with behaviors.<sup>4,7,17,19,62</sup> These

observations show that microdialysis provides valid and useful indices of neurochemical activity. Nevertheless, evidence of neurochemical instability over the postimplantation time window has been a long-standing issue in the field.

We hypothesize that mitigating disruption of the tissue near the probes would continue the refinement of intracranial microdialysis. To date, we have obtained encouraging results from the retrodialysis of dexamethasone (DEX), an anti-inflammatory drug, and XJB-5-131 (XJB), a novel scavenger of reactive oxygen species.<sup>43</sup> During acute experiments conducted 2–4 h after implanting microdialysis probes, both DEX and XJB diminished the loss in amplitude of evoked dopamine (DA) responses measured by fast-scan cyclic voltammetry (FSCV). Histochemical studies provide clear indications that DEX and XJB offer anti-inflammatory protection of the tissues surrounding the probes. Without DEX or XJB, the probes cause ischemia, disrupt endothelial cells, activate both astrocytes and microglia, and cause a loss in both neurons and axons near the probe tracks.<sup>43</sup> DEX was slightly more effective than XJB.<sup>43</sup> DEX retrodialysis for 5 days prevented the formation of a glial scar.<sup>41</sup>

We implanted microdialysis probes in the rat striatum for 4 and 24 h, both with and without DEX in the perfusion fluid,

**Special Issue:** Monitoring Molecules in Neuroscience 2014

**Received:** October 15, 2014

**Revised:** December 4, 2014

**Published:** December 10, 2014

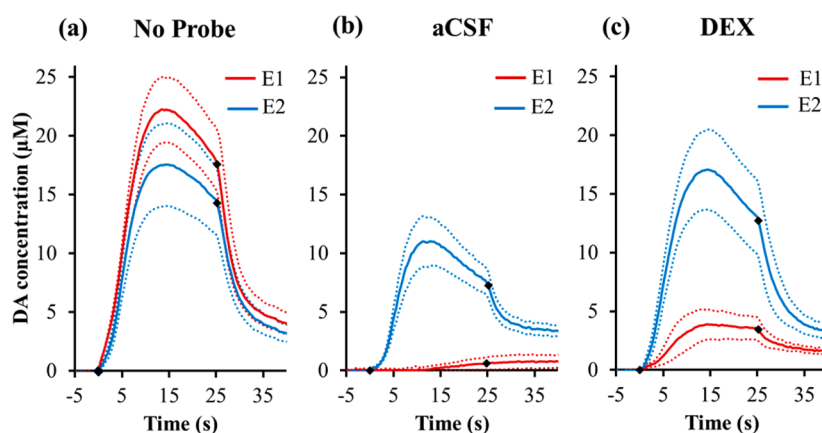


**Figure 1.** Evoked responses observed at the E1 (red) and E2 (blue) locations (a) with no microdialysis probe ( $n = 5$ ), (b) after 24 h perfusion with aCSF ( $n = 6$ ), and (c) after 24 h perfusion with DEX ( $n = 6$ ). The solid lines are the averages of the responses and the dotted lines are the SEMs. Black diamonds show when the stimulus begins and ends (see Figure 2 for statistics).

and then measured evoked DA release next to and at the outlet of the probes with FSCV. We report here for the first time that DEX significantly diminishes the loss in amplitude of evoked responses measured in the tissue next to the probe both at 4 and 24 h after implanting the probes. Responses at the probe outlet were below the detection limits of FSCV unless animals were treated with the DA uptake inhibitor, nomifensine, which increases the microdialysis recovery of evoked dopamine transients.<sup>59,63,64</sup> When probes were perfused without DEX, post-nomifensine responses at the probe outlet exhibited a significant decline in amplitude between 4 and 24 h postimplantation. However, DEX abolished this instability, both in animals treated first with nomifensine and then with raclopride. Thus, we report here for the first time that DEX stabilizes, but does not alter, evoked dopamine responses at the outlet of microdialysis probes. Surprisingly, DEX had no significant effect on two key tissue markers for dopamine terminals, tyrosine hydroxylase (TH) and the dopamine transporter (DAT): 24 h after probe implantation, these markers were not significantly different than that for control, nonimplanted tissues. We therefore attribute DEX's effects on evoked dopamine responses next to and at the outlet of microdialysis probes to its anti-inflammatory actions, as opposed to any direct actions on dopamine terminals. Finally, we report for the first time that the penetration of DEX into the tissue near the probe is extremely limited. Fluorescein-labeled DEX was found no further than 80  $\mu\text{m}$  from its delivery probe. Moreover, DEX failed to abolish gliosis near a second probe placed 2 mm from the probe with DEX. We therefore conclude that DEX's anti-inflammatory actions are tightly confined to the immediate, local vicinity of the probe.

## RESULTS AND DISCUSSION

**Characteristics of Evoked DA Release in the Rat Striatum.** Electrical stimulation of DA axons in the medial forebrain bundle (MFB) evokes DA release in the ipsilateral striatum, which is easily measurable by FSCV (Figure 1a).<sup>65–68</sup> We measured evoked dopamine responses both in the absence of microdialysis probes and with microelectrodes aimed 70–100  $\mu\text{m}$  (E1) and 1 mm (E2) from the probes (Figure S1, Supporting Information). In the absence of a microdialysis probe, there is no significant difference in the amplitude of evoked responses (45 Hz, 300  $\mu\text{A}$ , 25 s) measured at the E1 and E2 locations (Figures 1a and 2). The 24 h sham control

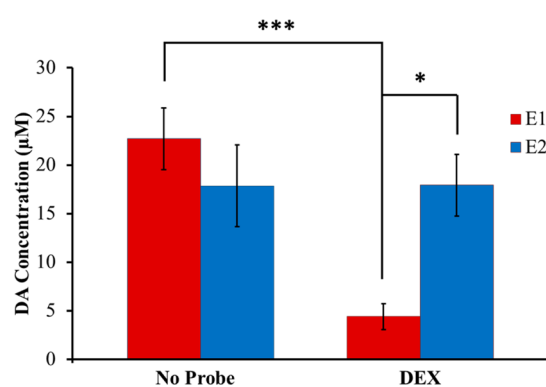


**Figure 2.** Summary of the amplitude of evoked responses (average  $\pm$  SEM) at the E1 (red) and E2 (blue) locations without microdialysis probes ( $n = 5$ ) and 24 h after probes were implanted and perfused with DEX ( $n = 6$ ). The evoked response at the E1 location after perfusion with aCSF was nondetectable, so the aCSF results were excluded from the statistical analysis. Statistical analysis was performed by two-way ANOVA with location (E1, E2, repeated measure) and probe (no probe, probe with DEX) as the factors. Location is not a significant factor ( $F(1,9) = 1.99, p > 0.05$ ). Probe is a significant factor ( $F(1,9) = 9.08, p < 0.05$ ). Interaction between factors is significant ( $F(1,9) = 8.91, p < 0.05$ ). Post hoc pairwise comparisons with Bonferroni corrections showed that in the presence of DEX the response amplitude at the E1 location is significantly smaller compared to the amplitude at E1 with no probe ( $***p < 0.0005$ ) and compared to the amplitude at E2 ( $*p < 0.05$ ). A separate one-sample  $t$  test shows that the response amplitude at E1 after 24 h of perfusion with DEX was significantly elevated above zero ( $t(5) = 3.33, p < 0.05$  (aCSF group)).

surgery (see Methods) had no significant effect on the response amplitudes measured at E1 (Figure S2).

**Voltammetry Next to the Probes.** We report here for the first time that evoked responses at the E1 location are abolished 24 h after implantation of microdialysis probes perfused with aCSF (Figure 1b, red line). This extends our prior acute study,<sup>43</sup> which showed that evoked responses were abolished 4 h after probe implantation. Together, these findings support previous evidence of neurochemical disruption of the tissue near probes over the 4–24 h postimplant interval,<sup>57,58</sup> when most microdialysis studies are performed.<sup>2,23,25,33</sup>

We report here for the first time that retrodialysis of DEX for 24 h diminishes, but does not eliminate, the loss in amplitude of

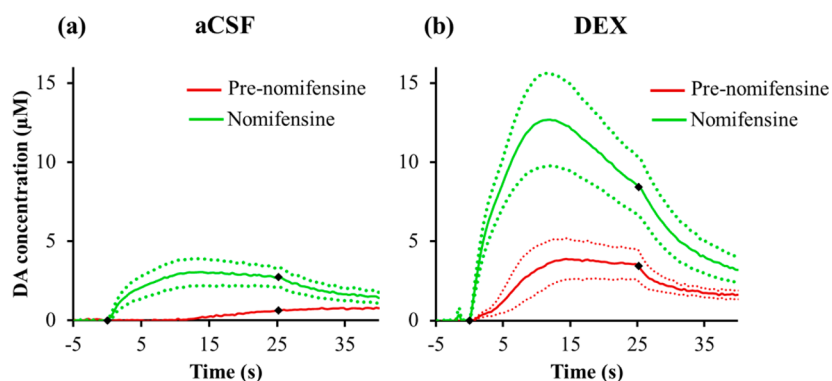


**Figure 3.** Nomifensine increases the amplitude of evoked responses at the E1 location (green = post-nomifensine, red = pre-nomifensine, responses in red are from Figure 2; solid lines = response averages, dotted lines = SEMs,  $n = 6$  per group; black diamonds indicate where the stimulus begins and ends).

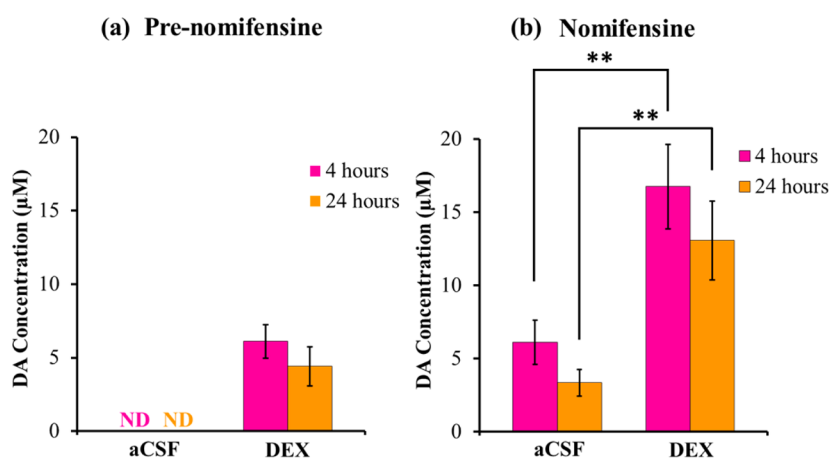


**Figure 4.** Summary of the amplitudes of evoked DA responses at the E1 location (average  $\pm$  SEM) observed 4 h (pink)<sup>43</sup> and 24 h (orange) after probe implantation (a) before and (b) after administration of nomifensine. In the absence of nomifensine, DA was nondetectable (ND) near probes perfused with aCSF, so statistical analysis was confined to the results obtained after nomifensine administration (panel b). Statistical analysis was by two-way ANOVA with time (4, 24 h) and perfusion condition (aCSF, DEX) as factors. Time is not a significant factor ( $F(1,20) = 2.22$ ,  $p > 0.05$ ). Perfusion condition is a significant factor ( $F(1,20) = 22.1$ ,  $p < 0.0005$ ). The interaction between factors was not significant ( $F(1,20) = 0.046$ ,  $p > 0.05$ ). Post hoc pairwise comparisons with Bonferroni correction show that DEX significantly increased the post-nomifensine responses at 4 and 24 h compared to those observed with aCSF (\*\* $p < 0.005$ ).

evoked responses at the E1 location (Figure 1c, red line). Evoked responses at the E1 location were significantly elevated compared to zero response, although they were significantly smaller than the responses at the E2 location (Figure 2, statistics reported in the figure legend). In the presence of DEX, there was no significant difference in the response amplitude at the E2 location compared to that observed in the absence of a probe (Figure 2). Thus, DEX offers partial protection of evoked responses at the E1 location without affecting the responses at the E2 location. The lack of significant effects at the E2 location suggests that the tissue disruption is confined to the tissue in close proximity to the probe.

DA reuptake affects the *in vivo* microdialysis recovery of DA.<sup>46,63,64</sup> Therefore, it is of interest to know how inhibition of the DA transporter (DAT) affects evoked DA responses next to the probes. Consistent with numerous reports in the absence of microdialysis probes,<sup>69–73</sup> nomifensine (20 mg/kg *i.p.*) increased the amplitude of evoked DA responses at the E1 location 24 h after implanting the probes (Figure 3, green lines). In the case of probes perfused with aCSF, nomifensine elevated the evoked response from below to above the detection limit of FSCV (Figure 3).

When probes were perfused for 4 or 24 h without DEX, evoked DA responses at the E1 location were nondetectable (Figure 4a). Therefore, we must rely on responses measured in nomifensine-treated animals to compare the effects of DEX at 4 and 24 h postimplantation (Figure 4b). Statistical analysis was by two-way ANOVA (details in the figure legend) with time (4 h, 24 h) and perfusion condition (aCSF, DEX) as factors with posthoc tests. The perfusion condition, but not time, was a significant factor (interaction was not significant). Thus, DEX significantly affected the response amplitudes and those amplitudes were stable between 4 and 24 h post implantation.

**Voltammetry at the Probe Outlet.** FSCV was performed at the outlet of microdialysis probes to quantify evoked responses in the dialysate stream (Figure S3). The stimulus parameters were identical to those used to obtain Figures 1–4 (45 Hz, 300  $\mu$ A, 25 s). The evoked responses are reported in Figure 5, in which the time axes have been adjusted to account for the time needed for the dialysate to flow from the probe to the end of the outlet line: the transit time was confirmed by calibration and agreed with calculated values. The vertical axes in Figure 5 were obtained by postcalibration of the detection electrode in a flow cell apparatus without correction for probe

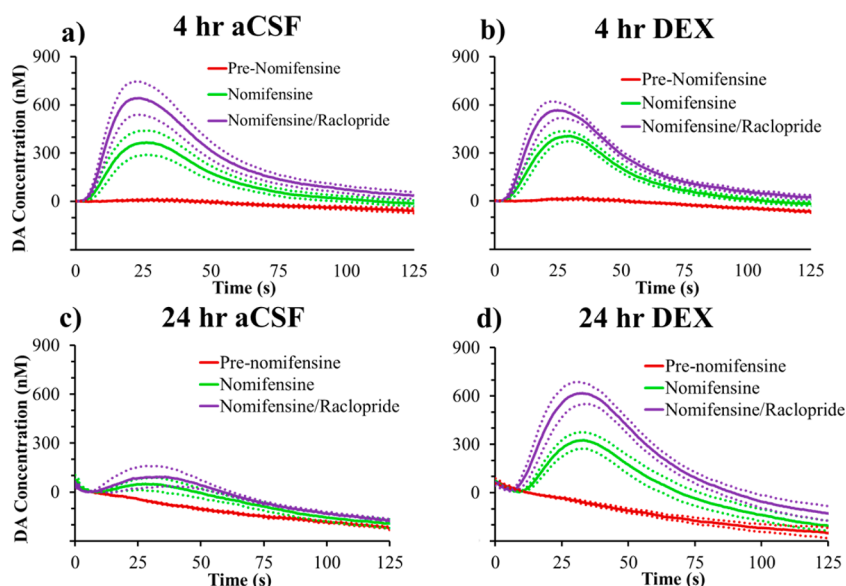


**Figure 5.** Effect of aCSF and DEX on the average ( $\pm$ SEM) evoked DA release measured at the probe outlet pre-nomifensine (red), after nomifensine (green), and after both nomifensine and raclopride (purple). Evoked release was measured (a, b) 4 h and (c, d) 24 h after probe implantation ( $n = 6$  per group). A negative dopamine concentration means that the current dropped below the baseline current response as a result of the baseline drift from the electrochemical pretreatment of the carbon fiber (see Methods and Supporting Information).

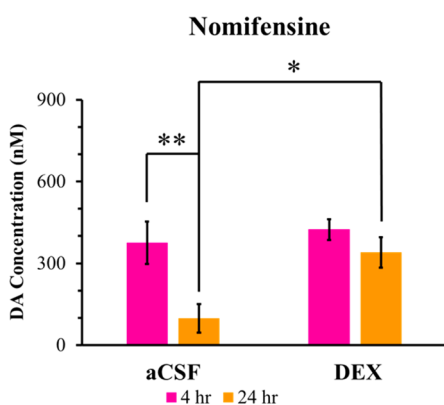


**Figure 6.** Average maximum evoked DA concentration ( $\pm$ SEM) observed at the outlet of microdialysis probes after nomifensine comparing 4 h (pink,  $n = 6$ ) and 24 h (orange,  $n = 6$ ) after probe implantation. In a two-way ANOVA time (4, 24 h),  $F(1,20) = 9.86$ ,  $p < 0.01$ , and treatment (aCSF, DEX),  $F(1,20) = 6.37$ ,  $p < 0.05$ , were significant effects on the DA concentration post-nomifensine. There was no significant interaction  $F(1,20) = 2.82$ ,  $p > 0.05$ . In a post hoc pairwise comparisons with Bonferroni corrections, there is a significant difference between aCSF at 4 and 24 h and between aCSF and DEX at 24 h. \* $p < 0.01$  and \*\* $p < 0.005$ .

recovery, so the vertical axes report dialysate, not in vivo, DA concentrations. The DA responses in Figure 5 exhibit some baseline drift: this is due to the electrode pretreatment strategy used to optimize the sensitivity of the electrodes (see Methods and Supporting Information).

Evoked DA release was nondetectable at the outlet of probes perfused with aCSF or DEX for 4 or 24 h (Figure 5, red lines). This is consistent with our prior experience that evoked DA responses at the probe outlet are below the detection limits of FSCV unless the DA uptake mechanism is inhibited.<sup>64,74,75</sup> This observation is consistent with the results of our measurements at the E1 location, described above. In the case of perfusion with aCSF, evoked responses are below FSCV

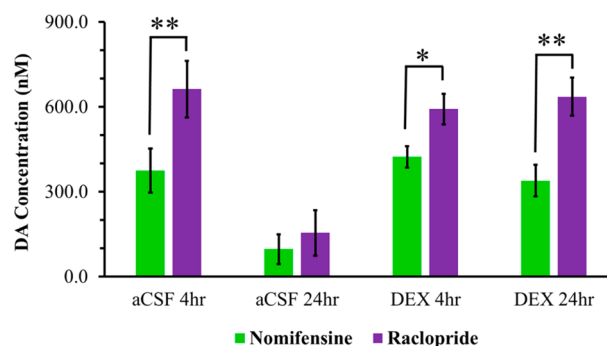


**Figure 7.** Average maximum evoked DA concentration ( $\pm$ SEM) collected by the probe. A three-way ANOVA with repeated measures was completed comparing the effects of time (4, 24 h), treatment (aCSF, DEX), and drug (nomifensine, raclopride). As seen in the nomifensine data, time  $F(1,20) = 10.4$ ,  $p < 0.005$ ; treatment  $F(1,20) = 7.52$ ,  $p < 0.05$ ; and now the interaction between treatment and time  $F(1,20) = 8.47$ ,  $p < 0.01$  are significant. The effect of drug (between nomifensine and raclopride) was significant  $F(1,20) = 74.7$ ,  $p < 0.0000005$ , and the interaction between time and treatment and drug was also significant  $F(1,20) = 14.5$ ,  $p < 0.05$ . A post hoc pairwise comparison with Bonferroni corrections shows a significant increase from nomifensine to raclopride in 3 of the 4 experiments. \* $p < 0.005$  and \*\* $p < 0.000005$ .

detection limits next to the probe, which explains why no response was detected at the probe outlet. DEX significantly increased the response amplitude at the E1 location but evidently, not sufficiently enough to produce a detectable response at the probe outlet.

Evoked DA release was detected at the probe outlet following administration of the dopamine uptake inhibitor, nomifensine (20 mg/kg i.p., Figure 5, green lines), consistent with the ability of nomifensine to increase evoked responses at the E1 location. In the case of probes perfused with aCSF, the post-nomifensine response was not stable: the response amplitude declined significantly between 4 and 24 h after implantation (Figure 6, statistics reported in figure legend). No



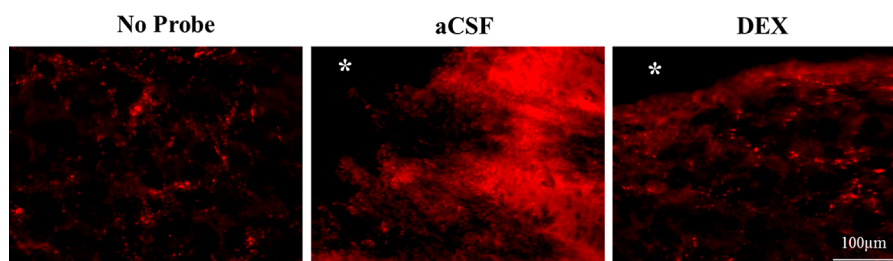


**Figure 8.** High magnification images (60 $\times$ ) of punctate TH labeling in control tissue (left), tissue near the tracks of probes perfused for 24 h with aCSF (middle) and DEX (right). Punctate TH labeling is diminished near probes perfused with aCSF, and diffuse TH labeling is increased. Control experiments did not indicate nonspecific binding, so the diffuse labeling is presumed to derive from specific binding. Punctate labeling is evident in the DEX image, which does not exhibit diffuse TH labeling. The asterisk near the top of the middle and right-hand images marks a portion of the probe track.

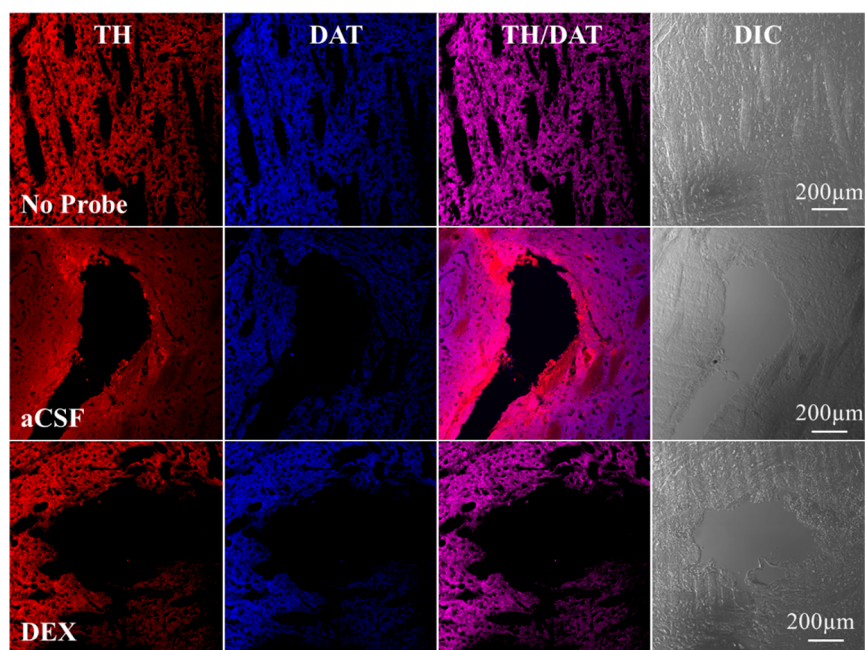


**Figure 9.** Separate rows illustrate representative fluorescent images of striatal tissue with no probe, or after retrodialysis of aCSF, or DEX for 24 h. Separate columns provide tissue (from left to right) labeled with TH, DAT, their respective overlaid images, and corresponding DIC images. Scale bars are 200  $\mu\text{m}$ .

such instability was observed at the E1 location, which suggests that responses are affected more closer to the probe, as we have previously suggested.<sup>57</sup> DEX eliminated this instability: in the presence of DEX, there was no significant difference in the responses at the probe outlet at 4 and 24 h postimplantation (Figure 6). Hence, we report here for the first time on DEX's ability to stabilize evoked responses at the probe outlet over the 4–24 h postimplantation interval.

The statistical analysis also shows there were no significant differences between the response amplitudes measured at the outlet of probes perfused with DEX and those perfused for 4 h with aCSF (Figure 6). Thus, DEX stabilized, but does appear to have altered, the responses at the probe outlet.

Following the administration of nomifensine, rats received a single dose of the D2 DA receptor antagonist, raclopride (2 mg/kg i.p.), and a final evoked response was measured at the probe outlet (Figure 5, purple lines). As expected,<sup>58,66,72,76</sup> the autoreceptor antagonist caused a further increase in the response amplitudes, as summarized in Figure 7. Statistical analysis of Figure 7 was by a mixed-model three-way ANOVA of time (4 h, 24 h), perfusion medium (aCSF, DEX), and drug

(nomifensine, raclopride, with repeated measure) as the main factors (details in the figure legend). The responses at the outlet of probes perfused with aCSF significantly diminished between 4 and 24 h postimplantation. There were no significant differences between the responses observed in the 4 h aCSF, 4 h DEX, and 24 h DEX cases: this shows that DEX stabilized but did not alter these responses. Raclopride significantly increased the evoked responses in the 4 h aCSF, 4 h DEX, and 24 h DEX cases but not in the 24 h aCSF case.

Thus, as judged on the basis of evoked responses measured at the outlet of microdialysis probes, DEX eliminated the instability in DA neurochemistry between 4 and 24 h post implantation in animals treated first with nomifensine and then with raclopride. Perfusion with aCSF for 24 h caused a loss in the significance of the effects of both nomifensine and raclopride combination. The loss in amplitude reported here is consistent with several prior reports of instability of DA following probe implantation.<sup>37,53,54,74</sup>

**Immunohistochemistry of the Probe Track.** We performed histochemical analysis of striatal tissues using antibodies for two widely accepted markers of DA terminals,

tyrosine hydroxylase (TH) and the DAT.<sup>77–79</sup> Nonimplanted, control tissue (contralateral to microdialysis probes) exhibits punctate TH labeling (Figure 8 left). Punctate labeling is diminished in images of tissue near the tracks of probes perfused with aCSF, which also exhibit diffuse TH labeling (Figure 8 middle): control experiments did not reveal nonspecific binding, which indicates that the diffuse labeling is specific binding. The exact cause of the diffuse labeling is unknown at this time but represents disruption of the tissue adjacent to the probe. Punctate, but not diffuse, labeling is clearly visible in the image of tissue near the track of a probe perfused with DEX (Figure 8 right). These images support the conclusion that DEX protects DA terminals near microdialysis probes.

At lower magnification (Figure 9), control tissue labeled for TH and DAT exhibited nonlabeled areas corresponding to myelinated axon bundles, which are also visible under differential interference contrast (DIC). The probe tracks are clearly visible (Figure 9, middle and bottom rows). Some diffuse labeling around probes perfused with aCSF is evident in the TH image (Figure 9, middle row): we have observed such binding before and consider it an edge effect.<sup>43,80</sup> Overall, TH and DAT labeling was clearly evident near the tracks of probes perfused both with and without DEX (quantification is discussed, below).

The intense TH labeling near probe tracks perfused with aCSF for 24 h stands in clear contrast to the absence of TH labeling that we observed 4 h after implantation.<sup>43</sup> The exact mechanism whereby this interesting rebound of TH labeling occurs is not yet known: possibilities, to be explored further in future studies, might include the synthesis of new TH protein by surviving DA terminals and/or the sprouting of new DA terminals.<sup>81,82</sup>

The TH and DAT images were converted to 2D intensity scatter plots (Figure 10a), from which we determined Pearson's correlation coefficient (PCC) and Manders' overlay coefficient (MOC) (see the Supporting Information for explanations of these coefficients).<sup>83</sup> The correlation coefficients in images with and without probe tracks are indistinguishable for probes perfused with DEX (Figure 10b). The correlation coefficients are only slightly reduced with aCSF compared to DEX, most likely due to the nonspecific edge effect.<sup>84</sup> Overall, the probes with DEX had no significant effect on the correlation of TH and DAT labeling in the nearby tissue (see Figure 10 legend). Regions of interest in the TH and DAT labeled images were defined to eliminate the probe track (for details, see Supporting Information Figure S4). There were no significant differences in the quantitative TH and DAT labeling in nonimplanted control tissue and the regions of interest around the tracks of probes perfused for 24 h with either aCSF or DEX (Figure 10c).

Overall, probe implantation had no significant effect on TH and DAT, two key markers for DA terminals. This supports our conclusion that DEX's effects on evoked responses are attributable to its previously documented anti-inflammatory actions,<sup>41,43</sup> as opposed to direct actions on DA terminals. Our prior studies show that DEX profoundly decreases ischemia, glial activation, and neuron loss in the tissues near microdialysis probes.<sup>41,43</sup> It appears that these actions are responsible for the effects of DEX on evoked DA responses next to and at the outlet of microdialysis probes over the 4–24 h post-implantation interval.

**Evaluating the Tissue Penetration and the Physical Extent of DEX's Anti-Inflammatory Actions.** First, we used fluorescein-labeled DEX (DEX-FL) to assess how far DEX

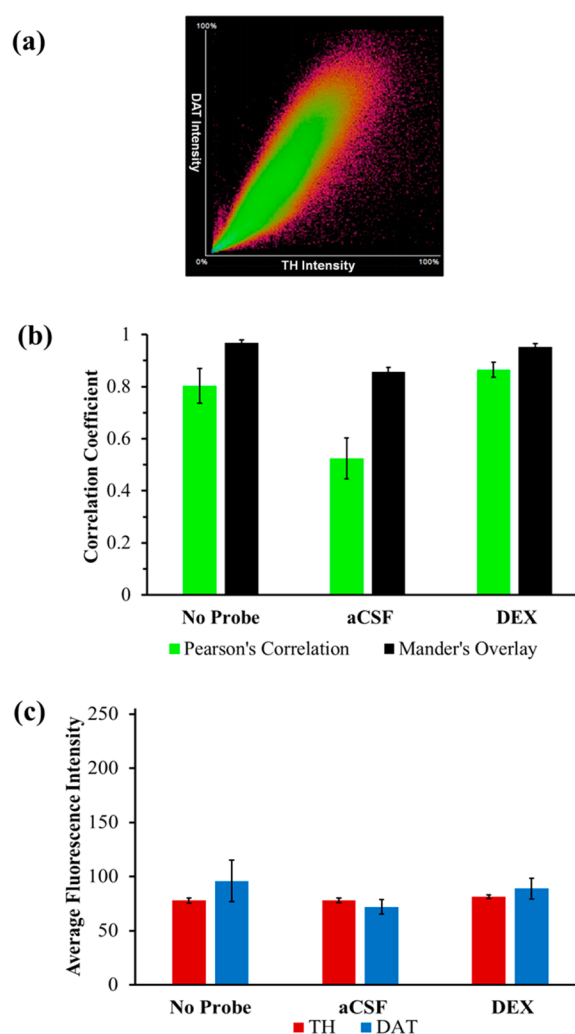


**Figure 10.** (a) Scatter plot of TH and DAT intensities. (b) Correlation coefficients between TH and DAT pixels among the three groups (no probe, aCSF and DEX,  $n = 3$  rats (total of 6 images per group)) for both Mander's overlay (black) and Pearson's correlation (green). A two-way ANOVA comparing the treatment (no probe, aCSF, and DEX) and analysis (Pearson's correlation and Mander's overlay) showed that there were significant differences in treatment  $F(2,28) = 14.2$ ,  $p < 0.0001$ , analysis  $F(1,28) = 29.7$ ,  $p < 0.00001$ , and the interaction treatment and analysis  $F(2,28) = 3.87$ ,  $p < 0.05$ . A post hoc Tukey test further showed aCSF correlation coefficients were significantly reduced compared to no probe ( $p < 0.0005$ ) and DEX ( $p < 0.0001$ ). A post hoc pairwise comparisons with Bonferroni corrections showed that Mander's overlay and Pearson's correlation differ from each other with no probes ( $p < 0.05$ ) and aCSF ( $p < 0.00005$ ). (c) Average fluorescent intensity for TH (red) and DAT (blue) for no probe, aCSF, and DEX ( $n = 3$  rats (total of 6 images per group)). Fluorescent intensity ranges from 0 to 255 with 255 being the highest value. In a two-way ANOVA comparing treatment (no probe, aCSF, and DEX,  $F(2,30) = 0.97$ ,  $p > 0.05$ ) and stain (TH and DAT,  $F(2,30) = 0.74$ ,  $p > 0.05$ ), there were no significant differences in average fluorescent intensity.

penetrates into the tissue near microdialysis probes. After 4 h of retrodialysis, DEX-FL penetrated only to  $78.6 \pm 46.1 \mu\text{m}$  from the probe track (Figure 11). This result, however, might be affected by the detection limit of the fluorescence measurement and possibly by loss of soluble DEX-FL during tissue processing. So, second, we performed dual-probe microdialysis experiments ( $n = 3$ ) with the probes implanted 2 mm apart.

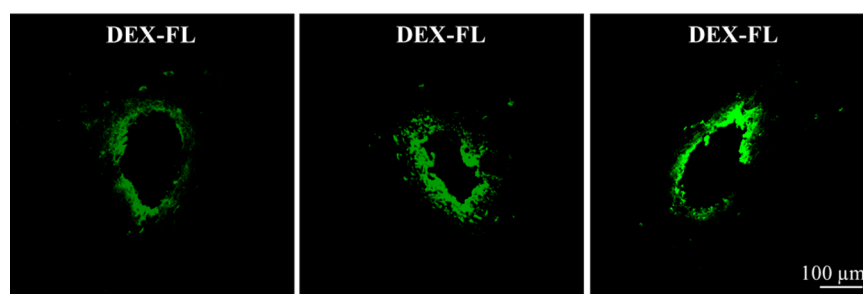


**Figure 11.** Images of the microdialysis probe track, from three different rats, after 4 h perfusion of DEX-FL. DEX-FL is delivered locally only to the tissue directly surrounding the probe.

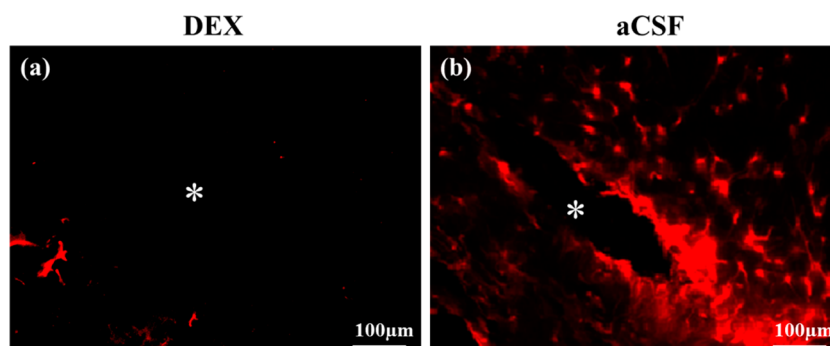


**Figure 12.** Fluorescently labeled GFAP images (a) with and (b) without DEX. Retrodialysis was performed for 24 h in striatal tissue. The asterisks indicate the center of the probe tracks.

One probe was perfused with DEX for 24 h, and the other with aCSF. DEX abolished gliosis, as measured with GFAP, near the probe with DEX but not near the probe 2 mm away (Figure 12). We therefore conclude that DEX does not penetrate deeply into brain tissue and that its actions are confined to within close proximity to the delivery probe.

## CONCLUSIONS

Our findings reiterate that tissue damage occurs when a microdialysis probe is implanted into brain tissue.<sup>38–44</sup> The extent of damage is documented to be sufficient to cause time-dependent neurochemical and histological disruptions in the tissue next to the probes over the 4–24 h postimplant interval, a typical time frame for microdialysis studies.<sup>2,23,25,33</sup> Here, based on the properties of evoked DA responses measured next to and at the outlet of microdialysis probes and on histological findings, we have documented for the first time that DEX offers protective mitigation against such disruptions over the 4–24 h time interval following probe implantation. The actions of DEX reported here appear to derive from its previously documented anti-inflammatory actions,<sup>41,43</sup> rather than any direct neurochemical action on DA terminals per se. We have also documented here a surprising rebound of TH labeling in the tissue surrounding probe tracks by 24 h postimplantation: this might indicate the presence of surviving DA terminals, which justifies our efforts to protect and preserve their neurochemical activity. Finally, we document here for the first time that the actions of DEX are tightly confined to the immediate, local vicinity of the microdialysis probe used for delivery.

## METHODS

The methods used during this study have been described previously.<sup>40–43,57,58,64</sup> We provide key details here and full descriptions in the Supporting Information.

**Reagents and Solutions.** All solutions were prepared with ultrapure water (Nanopure, Barnstead, Dubuque, IA). All reagents were used as received from their suppliers. Artificial cerebrospinal fluid (aCSF: 142 mM NaCl, 1.2 mM CaCl<sub>2</sub>, 2.7 mM KCl, 1.0 mM MgCl<sub>2</sub>, 2.0 mM NaH<sub>2</sub>PO<sub>4</sub>, pH 7.4) was the perfusion fluid for microdialysis. DEX sodium phosphate (DEX, APP Pharmaceuticals LLC Schaumburg, IL) was diluted to 10 μM in aCSF. This dose was used as we have previously observed a dramatic reduction in tissue disruption at 10 μM DEX for 24 h.<sup>41</sup> DEX fluorescein (DEX-FL, Life Technologies Grand Island, NY) was diluted to 10 μM in aCSF. Nomifensine maleate and *S*(-)-raclopride (+)-tartrate salts (Sigma-Aldrich, St. Louis, MO) were dissolved in phosphate-buffered saline (PBS: 155 mM NaCl, 100 mM NaH<sub>2</sub>PO<sub>4</sub>, pH 7.40) and administered at 20 mg/kg (i.p.) and 2 mg/kg (i.p.), respectively. Isopropyl alcohol (Sigma-Aldrich, St. Louis, MO) and decolorizing carbon (Fisher, Pittsburgh, PA) were used to pretreat carbon fiber electrodes for DA voltammetry. DA (Sigma-Aldrich, St. Louis, MO) standards were prepared in N<sub>2</sub>-purged aCSF.

**Microdialysis Probes.** Concentric microdialysis probes (300 μm diameter, 4 mm length) were constructed with hollow fiber membranes (13 kDa MWCO, Spectra/Por RC, Spectrum Laboratories Inc., Ranco Dominguez, CA). The inlet tubing (PE, Becton Dickinson, Franklin Lakes, NJ) was connected to a 1 mL gastight syringe driven by a microliter syringe pump (Harvard Apparatus, Holliston, MA) at a rate of 0.610 μL/min. The outlet was a fused silica capillary (75 μM I.D., 150 μM O.D., 10 cm long; Polymicro Technologies, Phoenix, AZ). Probes were perfused with either aCSF or aCSF containing 10 μM DEX.

**Microdialysis Probe Implantation.** All procedures involving animals were approved by the University of Pittsburgh's Animal Care and Use Committee. Male Sprague–Dawley rats (250–350 g; Hilltop, Scottsdale, PA) underwent sterile stereotaxic surgery under isoflurane anesthesia. The probes were lowered into the brain at 5 μm/s with an automated micropositioner (model 2660, David Kopf Instruments, Tujunga, CA) and secured to the skull with screws and acrylic cement. Following surgery, the rats were placed in a Ratan microdialysis bowl (MD-1404, BASI, West Lafayette, IN) and the probes were perfused with aCSF or DEX for 24 h.



**Voltammetry Next to Microdialysis Probes.** Voltammetry next to microdialysis probes was performed in two groups of rats ( $n = 6$  rats per group). An additional control group ( $n = 5$ ) underwent an initial surgical procedure without probe implantation (a sham control). Four-hour maximum dopamine amplitudes previously collected<sup>43</sup> were used for probe temporal comparisons (Figure 4, 4 h results).

After spending 24 h in the Return bowl, the rats were anesthetized a second time and returned to the stereotaxic frame. A carbon fiber electrode (400  $\mu\text{m}$  in length) was implanted in the same coronal plane as the probe. As before,<sup>43</sup> the electrode was aimed at an angle of  $5^\circ$  from vertical so that it could be placed very close to the probe. At its final location, the tip of the carbon fiber was 70  $\mu\text{m}$  and the base of the fiber (where it meets the tip of the glass capillary) was 100  $\mu\text{m}$  from the probe: we call this the E1 location (Figure S1). A second carbon fiber was aimed vertically 1 mm posterior to and in the same sagittal plane as the probe: we call this the E2 location (Figure S1). The relative position of the two carbon fibers to the probe is based on the adjustments made using stereotaxic micropositioners (10  $\mu\text{m}$ ) resolution.<sup>43</sup> The exact distance between the two electrodes and the probe cannot be determined accurately without an electrolytic lesion which would not allow postcalibration of the electrodes. Variations in the relative positions of the electrodes and probe contribute to the standard deviations of the results.

A stimulating electrode was lowered toward the MFB until evoked DA was detected at E2 (stimulus waveform: biphasic, square, constant current). The parameters for subsequent stimuli are listed in the Results and Discussion.

**Voltammetry at the Probe Outlet.** Voltammetry at the probe outlet was performed in a custom-made Plexiglas detection chamber (Figure S3). A carbon fiber electrode (800  $\mu\text{m}$  long) was inserted into the end of the capillary outlet line with a miniature micromanipulator (Fine Science Tools, Foster City, CA). As described previously,<sup>64</sup> the electrodes were electrochemically pretreated 10 min before each stimulus or calibration procedure.

Voltammetry at the outlet was performed in four groups of rats, 4 or 24 h ( $n = 6$  per group) after probe implantation, with perfusion of aCSF or DEX. Animals in the 4 h group remained under isoflurane anesthesia throughout the experiment.

**Tissue Immunohistochemistry.** After the *in vivo* measurements, the rats were deeply anesthetized and the brain tissues were collected for immunohistochemical analysis.<sup>40</sup> Thin horizontal sections (35  $\mu\text{m}$ ) were cut in a cryostat at  $-21$  to  $-22^\circ\text{C}$  and labeled together with antibody for tyrosine hydroxylase (TH; 1:1000, Millipore, Temecula, CA) and the DA transporter (DAT; 1:400, Synaptic Systems, Göttingen, Germany). The secondary antibody was goat anti-rabbit IgG-Cy3 or IgG-Cy5 (Invitrogen, Eugene, OR). In another group of rats, probes perfused with DEX-FL were implanted for 4 h. Tissue processing details can be found in the Supporting Information. In an additional group of rats, two probes were implanted 2 mm apart, one perfused with aCSF and the other perfused with DEX for 24 h. Tissue sections (30  $\mu\text{m}$ ) were then stained with antibodies for GFAP (BD Biosciences Pharmingen, San Diego, CA). Fluorescence and optical differential interference contrast (DIC) images were acquired with an Olympus BX61 microscope (Olympus; Melville, NY) equipped with a 20 $\times$  objective. Nonimplanted tissue (from the hemisphere opposite the microdialysis probe) was used as control tissue. Quantitative image analysis was performed with NIS-Elements Advanced Research version 4.00 software (Nikon Instruments Inc., Melville, NY). See Figure S5 for further details.

**Statistics.** IBM Statistical Package for the Social Sciences (SPSS) 22 software was used for all statistical analysis.

## ■ ASSOCIATED CONTENT

### ● Supporting Information

Additional information as noted in text. The Supporting Information methods section expands on experimental details mentioned in the text including fast scan cyclic voltammetry procedures, animal and surgical procedures and immunohistochemistry and tissue processing details. Figure S1 is a

schematic of device placement for voltammetry near microdialysis probes. Figure S2 compares the maximum average evoked dopamine after rats underwent one or two surgeries. Figure S3 is a schematic for voltammetry at the microdialysis probe outlet. Figure S4 represents an example of the thresholding process by NIS Element Advanced Research software. Figure S5 illustrates the labeling scheme of striatal tissue with TH and DAT stains. This material is available free of charge via the Internet at <http://pubs.acs.org>.

## ■ AUTHOR INFORMATION

### Corresponding Author

\*Mailing address: University of Pittsburgh, Dept. of Chemistry, 219 Parkman Ave., Pittsburgh, PA 15260, USA. E-mail: [amichael@pitt.edu](mailto:amichael@pitt.edu). Phone: 412-624-8560.

### Funding

This work was funded by the NIH (NS 081744).

### Notes

The authors declare no competing financial interest.

### Author Contributions

Kathryn M. Nesbitt designed, conducted, and analyzed experiments involving voltammetry next to microdialysis probes at the E1 and E2 locations and co-wrote the manuscript. Erika L. Varner conducted and analyzed voltammetry at the microdialysis probe outlet experiments and co-wrote the manuscript. Andrea Jaquins-Gerstl performed and analyzed tissue immunohistochemistry of the microdialysis probe tract and co-wrote the manuscript. Adrian C. Michael secured funding, contributed to the experimental design and co-wrote the manuscript.

## ■ ABBREVIATIONS

DA, dopamine; DEX, dexamethasone; XJB, XJB-5-131; MFB, medial forebrain bundle; FSCV, fast-scan cyclic voltammetry; aCSF, artificial cerebrospinal fluid; TH, tyrosine hydroxylase; DAT, dopamine transporter; DIC, differential interference contrast; PCC, Pearson's correlation coefficient; MOC, Manders' overlay coefficient; DEX-FL, dexamethasone fluorescein; GFAP, glial fibrillary acidic protein

## ■ REFERENCES

- (1) Ungerstedt, U. (1984) Measurement of neurotransmitter release by intracranial dialysis. In *In Measurement of Neurotransmitter Release In Vivo* (Marsden, C. A., Ed.), pp 81–105, John Wiley & Sons, New York.
- (2) Westerink, B. H., and De Vries, J. B. (1988) Characterization of *in vivo* dopamine release as determined by brain microdialysis after acute and subchronic implantations: methodological aspects. *J. Neurochem.* 51, 683–687.
- (3) Feuerstein, D., Manning, A., Hashemi, P., Bhatia, R., Fabricius, M., Toliás, C., Pahl, C., Ervine, M., Strong, A. J., and Boutelle, M. G. (2010) Dynamic metabolic response to multiple spreading depolarizations in patients with acute brain injury: An online microdialysis study. *J. Cereb. Blood Flow Metab.* 30, 1343–1355.
- (4) Badiani, A., Oates, M. M., Day, H. E., Watson, S. J., Akil, H., and Robinson, T. E. (1998) Amphetamine-induced behavior, dopamine release, and *c-fos* mRNA expression: Modulation by environmental novelty. *J. Neurosci.* 18, 10579–10593.
- (5) El Arfani, A., Bentea, E., Aourz, N., Ampe, B., De Deurwaerdere, P., Van Eeckhaut, A., Massie, A., Sarre, S., Smolders, I., and Michotte, Y. (2014) NMDA receptor antagonism potentiates the L-DOPA-induced extracellular dopamine release in the subthalamic nucleus of hemi-parkinson rats. *Neuropharmacology* 85, 198–205.



- (6) Sharp, T., Maidment, N. T., Brazell, M. P., Zetterstrom, T., Ungerstedt, U., Bennett, G. W., and Marsden, C. A. (1984) Changes in monoamine metabolites measured by simultaneous in vivo differential pulse voltammetry and intracerebral dialysis. *Neuroscience* 12, 1213–1221.
- (7) Sharp, T., Zetterström, T., Ljungberg, T., and Ungerstedt, U. (1987) A direct comparison of amphetamine-induced behaviours and regional brain dopamine release in the rat using intracerebral dialysis. *Brain Res.* 401, 322–330.
- (8) Di Chiara, G., Tanda, G., and Carboni, E. (1996) Estimation of in-vivo neurotransmitter release by brain microdialysis: the issue of validity. *Behav. Pharmacol.* 7, 640–657.
- (9) Bosche, B., Dohmen, C., Graf, R., Neveling, M., Staub, F., Kracht, L., Sobesky, J., Lehnhardt, F. G., and Heiss, W. D. (2003) Extracellular concentrations of non-transmitter amino acids in peri-infarct tissue of patients predict malignant middle cerebral artery infarction. *Stroke* 34, 2908–2913.
- (10) Tossman, U., Eriksson, S., Delin, A., Hagenfeldt, L., Law, D., and Ungerstedt, U. (1983) Brain amino acids measured by intracerebral dialysis in portacaval shunted rats. *J. Neurochem.* 41, 1046–1051.
- (11) Wright, I. K., Upton, N., and Marsden, C. A. (1992) Effect of established and putative anxiolytics on extracellular 5-HT and 5-HIAA in the ventral hippocampus of rats during behaviour on the elevated X-maze. *Psychopharmacology (Berlin, Ger.)* 109, 338–346.
- (12) Westerink, B. H. (1995) Brain microdialysis and its application for the study of animal behaviour. *Behav. Brain Res.* 70, 103–124.
- (13) Carboni, E., Spielesoy, C., Vacca, C., Nosten-Bertrand, M., Giros, B., and Di Chiara, G. (2001) Cocaine and amphetamine increase extracellular dopamine in the nucleus accumbens of mice lacking the dopamine transporter gene. *J. Neurosci.* 21, 141–144 Rcl141.
- (14) Di Chiara, G., and Imperato, A. (1988) Drugs abused by humans preferentially increase synaptic dopamine concentrations in the mesolimbic system of freely moving rats. *Proc. Natl. Acad. Sci. U. S. A.* 85, 5274–5278.
- (15) Arbuthnot, G. W., Fairbrother, I. S., and Butcher, S. P. (1990) Brain microdialysis studies on the control of dopamine release and metabolism in vivo. *J. Neurosci. Methods.* 34, 73–81.
- (16) Zetterström, T., Sharp, T., Marsden, C. A., and Ungerstedt, U. (1983) In Vivo Measurement of Dopamine and Its Metabolites by Intracerebral Dialysis: Changes After d-Amphetamine. *J. Neurochem.* 41, 1769–1773.
- (17) Robinson, T. E., and Justice, J. B., Eds. (1991) *Techniques in the Behavioral and Neural Sciences, Vol. 7: Microdialysis in the Neurosciences*, Elsevier, Amsterdam.
- (18) Abercrombie, E. D., and Zigmond, M. J. (1989) Partial injury to central noradrenergic neurons: reduction of tissue norepinephrine content is greater than reduction of extracellular norepinephrine measured by microdialysis. *J. Neurosci.* 9, 4062–4067.
- (19) Westerink, B. H., and Cremers, T. I. F. H., Eds, (2007) *Handbook of Microdialysis: Methods, Applications and Perspectives*, Academic Press, London.
- (20) Kehr, J. (2006) New methodological aspects of microdialysis. In *Handbook of Behavioral Neuroscience* (Ben, H. C. W., and Thomas, I. F. H. C., Eds.), pp 111–129, Elsevier, Amsterdam.
- (21) Davies, M. I., Cooper, J. D., Desmond, S. S., Lunte, C. E., and Lunte, S. M. (2000) Analytical considerations for microdialysis sampling. *Adv. Drug Delivery Rev.* 45, 169–188.
- (22) Chefer, V. I., Thompson, A. C., Zapata, A., and Shippenberg, T. S. (2001) Overview of Brain Microdialysis. In *Current Protocols in Neuroscience*; John Wiley & Sons, Inc., New York.
- (23) Watson, C. J., Venton, B. J., and Kennedy, R. T. (2006) In Vivo Measurements of Neurotransmitters by Microdialysis Sampling. *Anal. Chem.* 78, 1391–1399.
- (24) Lee, W. H., Slaney, T. R., Hower, R. W., and Kennedy, R. T. (2013) Microfabricated sampling probes for in vivo monitoring of neurotransmitters. *Anal. Chem.* 85, 3828–3831.
- (25) Shou, M., Ferrario, C. R., Schultz, K. N., Robinson, T. E., and Kennedy, R. T. (2006) Monitoring dopamine in vivo by microdialysis sampling and on-line CE-laser-induced fluorescence. *Anal. Chem.* 78, 6717–6725.
- (26) Emmett, M. R., Andren, P. E., and Caprioli, R. M. (1995) Specific molecular mass detection of endogenously released neuropeptides using in vivo microdialysis/mass spectrometry. *J. Neurosci. Methods.* 62, 141–147.
- (27) Scott, D. E., Grigsby, R. J., and Lunte, S. M. (2013) Microdialysis sampling coupled to microchip electrophoresis with integrated amperometric detection on an all-glass substrate. *Chem-PhysChem* 14, 2288–2294.
- (28) Bert, L., Parrot, S., Robert, F., Desvignes, C., Denoroy, L., Suaud-Chagny, M. F., and Renaud, B. (2002) In vivo temporal sequence of rat striatal glutamate, aspartate and dopamine efflux during apomorphine, nomifensine, NMDA and PDC in situ administration. *Neuropharmacology* 43, 825–835.
- (29) Santiago, M., and Westerink, B. H. (1990) Characterization of the in vivo release of dopamine as recorded by different types of intracerebral microdialysis probes. *Naunyn-Schmiedeberg's Arch. Pharmacol.* 342, 407–414.
- (30) Parrot, S., Bert, L., Mouly-Badina, L., Sauvnet, V., Colussi-Mas, J., Lambas-Senas, L., Robert, F., Bouilloux, J. P., Suaud-Chagny, M. F., Denoroy, L., and Renaud, B. (2003) Microdialysis monitoring of catecholamines and excitatory amino acids in the rat and mouse brain: recent developments based on capillary electrophoresis with laser-induced fluorescence detection—a mini-review. *Cell. Mol. Neurobiol.* 23, 793–804.
- (31) Li, Q., Zubieta, J. K., and Kennedy, R. T. (2009) Practical aspects of in vivo detection of neuropeptides by microdialysis coupled off-line to capillary LC with multistage MS. *Anal. Chem.* 81, 2242–2250.
- (32) Zhang, J., Jaquins-Gerstl, A., Nesbitt, K. M., Rutan, S. C., Michael, A. C., and Weber, S. G. (2013) In vivo monitoring of serotonin in the striatum of freely moving rats with one minute temporal resolution by online microdialysis-capillary high-performance liquid chromatography at elevated temperature and pressure. *Anal. Chem.* 85, 9889–9897.
- (33) Yang, H., Thompson, A. B., McIntosh, B. J., Altieri, S. C., and Andrews, A. M. (2013) Physiologically Relevant Changes in Serotonin Resolved by Fast Microdialysis. *ACS Chem. Neurosci.* 4, 790–798.
- (34) Hopwood, S. E., Parkin, M. C., Bezzina, E. L., Boutelle, M. G., and Strong, A. J. (2005) Transient changes in cortical glucose and lactate levels associated with peri-infarct depolarizations, studied with rapid-sampling microdialysis. *J. Cereb. Blood Flow Metab.* 25, 391–401.
- (35) Tang, A., Bungay, P. M., and Gonzales, R. A. (2003) Characterization of probe and tissue factors that influence interpretation of quantitative microdialysis experiments for dopamine. *J. Neurosci. Methods* 126, 1–11.
- (36) Zhou, F., Braddock, J. F., Hu, Y., Zhu, X., Castellani, R. J., Smith, M. A., and Drew, K. L. (2002) Microbial origin of glutamate, hibernation and tissue trauma: An in vivo microdialysis study. *J. Neurosci. Methods.* 119, 121–128.
- (37) Holson, R. R., Gazzara, R. A., and Gough, B. (1998) Declines in stimulated striatal dopamine release over the first 32 h following microdialysis probe insertion: generalization across releasing mechanisms. *Brain Res.* 808, 182–189.
- (38) Benveniste, H., and Diemer, N. H. (1987) Cellular reactions to implantation of a microdialysis tube in the rat hippocampus. *Acta Neuropathol.* 74, 234–238.
- (39) Clapp-Lilly, K. L., Roberts, R. C., Duffy, L. K., Irons, K. P., Hu, Y., and Drew, K. L. (1999) An ultrastructural analysis of tissue surrounding a microdialysis probe. *J. Neurosci. Methods* 90, 129–142.
- (40) Jaquins-Gerstl, A., and Michael, A. C. (2009) Comparison of the brain penetration injury associated with microdialysis and voltammetry. *J. Neurosci. Methods* 183, 127–135.
- (41) Jaquins-Gerstl, A., Shu, Z., Zhang, J., Liu, Y., Weber, S. G., and Michael, A. C. (2011) Effect of dexamethasone on gliosis, ischemia, and dopamine extraction during microdialysis sampling in brain tissue. *Anal. Chem.* 83, 7662–7667.

- (42) Mitala, C. M., Wang, Y., Borland, L. M., Jung, M., Shand, S., Watkins, S., Weber, S. G., and Michael, A. C. (2008) Impact of microdialysis probes on vasculature and dopamine in the rat striatum: A combined fluorescence and voltammetric study. *J. Neurosci. Methods* 174, 177–185.
- (43) Nesbitt, K. M., Jaquins-Gerstl, A., Skoda, E. M., Wipf, P., and Michael, A. C. (2013) Pharmacological Mitigation of Tissue Damage during Brain Microdialysis. *Anal. Chem.* 85, 8173–8179.
- (44) Zhou, F., Zhu, X., Castellani, R. J., Stimmelmayer, R., Perry, G., Smith, M. A., and Drew, K. L. (2001) Hibernation, a model of neuroprotection. *Am. J. Pathol.* 158, 2145–2151.
- (45) Hascup, E. R., af Bjerken, S., Hascup, K. N., Pomerleau, F., Huettl, P., Stromberg, I., and Gerhardt, G. A. (2009) Histological studies of the effects of chronic implantation of ceramic-based microelectrode arrays and microdialysis probes in rat prefrontal cortex. *Brain Res.* 1291, 12–20.
- (46) Bungay, P. M., Newton-Vinson, P., Isele, W., Garris, P. A., and Justice, J. B. (2003) Microdialysis of dopamine interpreted with quantitative model incorporating probe implantation trauma. *J. Neurochem.* 86, 932–946.
- (47) Major, O., Shdanova, T., Duffek, L., and Nagy, Z. (1990) Continuous monitoring of blood-brain barrier opening to Cr51-EDTA by microdialysis following probe injury. *Acta Neurochir. Suppl. (Wien)* 51, 46–48.
- (48) Planas, A. M., Justicia, C., Sole, S., Friguls, B., Cervera, A., Adell, A., and Chamorro, A. (2002) Certain Forms of Matrix Metalloproteinase-9 Accumulate in the Extracellular Space After Microdialysis Probe Implantation and Middle Cerebral Artery Occlusion/Reperfusion. *J. Cereb. Blood Flow Metab.* 22, 918–925.
- (49) Kadota, E., Nonaka, K., Karasuno, M., Nishi, K., Nakamura, Y., Namikawa, K., Okazaki, Y., Teramura, K., and Hashimoto, S. (1994) Experimental quantitative evaluation of transvascular removal of unnecessary substances in brain edema fluid. *Acta Neurochir. Suppl. (Wien)* 60, 162–164.
- (50) Benveniste, H., Drejer, J., Schousboe, A., and Diemer, N. H. (1987) Regional cerebral glucose phosphorylation and blood flow after insertion of a microdialysis fiber through the dorsal hippocampus in the rat. *J. Neurochem.* 49, 729–734.
- (51) Davalos, D., Grutzendler, J., Yang, G., Kim, J. V., Zuo, Y., Jung, S., Littman, D. R., Dustin, M. L., and Gan, W. B. (2005) ATP mediates rapid microglial response to local brain injury in vivo. *Nat. Neurosci.* 8, 752–758.
- (52) Groothuis, J., Ramsey, N. F., Ramakers, G. M., and van der Plasse, G. (2014) Physiological challenges for intracortical electrodes. *Brain. Stimul.* 7, 1–6.
- (53) Holson, R. R., Bowyer, J. F., Clausing, P., and Gough, B. (1996) Methamphetamine-stimulated striatal dopamine release declines rapidly over time following microdialysis probe insertion. *Brain Res.* 739, 301–307.
- (54) Robinson, T. E., and Camp, D. M. (1991) The effects of four days of continuous striatal microdialysis on indices of dopamine and serotonin neurotransmission in rats. *J. Neurosci. Methods.* 40, 211–222.
- (55) Westerink, B. H., and Tuinte, M. H. (1986) Chronic use of intracerebral dialysis for the in vivo measurement of 3,4-dihydroxyphenylethylamine and its metabolite 3,4-dihydroxyphenylacetic acid. *J. Neurochem.* 46, 181–185.
- (56) Imperato, A., and Di Chiara, G. (1985) Dopamine release and metabolism in awake rats after systemic neuroleptics as studied by trans-striatal dialysis. *J. Neurosci.* 5, 297–306.
- (57) Borland, L. M., Shi, G., Yang, H., and Michael, A. C. (2005) Voltammetric study of extracellular dopamine near microdialysis probes acutely implanted in the striatum of the anesthetized rat. *J. Neurosci. Methods* 146, 149–158.
- (58) Wang, Y., and Michael, A. C. (2012) Microdialysis probes alter presynaptic regulation of dopamine terminals in rat striatum. *J. Neurosci. Methods* 208, 34–39.
- (59) Church, W. H., Justice, J. B., Jr., and Byrd, L. D. (1987) Extracellular dopamine in rat striatum following uptake inhibition by cocaine, nomifensine and bsztoprine. *Eur. J. Pharmacol.* 139, 345–348.
- (60) Pontieri, F. E., Tanda, G., and Di Chiara, G. (1995) Intravenous cocaine, morphine, and amphetamine preferentially increase extracellular dopamine in the “shell” as compared with the “core” of the rat nucleus accumbens. *Proc. Natl. Acad. Sci. U. S. A.* 92, 12304–12308.
- (61) Rahman, S., Zhang, J., Engleman, E. A., and Corrigan, W. A. (2004) Neuroadaptive changes in the mesoaccumbens dopamine system after chronic nicotine self-administration: A microdialysis study. *Neuroscience* 129, 415–424.
- (62) Lam, H. A., Wu, N., Cely, I., Kelly, R. L., Hean, S., Richter, F., Magen, I., Cepeda, C., Ackerson, L. C., Walwyn, W., Masliah, E., Chesselet, M. F., Levine, M. S., and Maidment, N. T. (2011) Elevated tonic extracellular dopamine concentration and altered dopamine modulation of synaptic activity precede dopamine loss in the striatum of mice overexpressing human alpha-synuclein. *J. Neurosci. Res.* 89, 1091–1102.
- (63) Floresco, S. B., West, A. R., Ash, B., Moore, H., and Grace, A. A. (2003) Afferent modulation of dopamine neuron firing differentially regulates tonic and phasic dopamine transmission. *Nat. Neurosci.* 6, 968–973.
- (64) Lu, Y., Peters, J. L., and Michael, A. C. (1998) Direct comparison of the response of voltammetry and microdialysis to electrically evoked release of striatal dopamine. *J. Neurochem.* 70, 584–593.
- (65) Garris, P. A., Christensen, J. R., Rebec, G. V., and Wightman, R. M. (1997) Real-time measurement of electrically evoked extracellular dopamine in the striatum of freely moving rats. *J. Neurochem.* 68, 152–161.
- (66) Moquin, K. F., and Michael, A. C. (2009) Tonic autoinhibition contributes to the heterogeneity of evoked dopamine release in the rat striatum. *J. Neurochem.* 110, 1491–1501.
- (67) Chang, S. Y., Kimble, C. J., Kim, I., Paek, S. B., Kressin, K. R., Boesche, J. B., Whitlock, S. V., Eaker, D. R., Kasasbeh, A., Horne, A. E., Blaha, C. D., Bennet, K. E., and Lee, K. H. (2013) Development of the Mayo Investigational Neuromodulation Control System: Toward a closed-loop electrochemical feedback system for deep brain stimulation. *J. Neurosurg.* 119, 1556–1565.
- (68) Amos, A. N., Roberts, J. G., Lingjiao, Q., Sombers, L. A., and McCarty, G. S. (2014) Reducing the Sampling Rate of Biochemical Measurements Using Fast-Scan Cyclic Voltammetry for In Vivo Applications. *IEEE Sens. J.* 14, 2975–2980.
- (69) Taylor, I. M., Jaquins-Gerstl, A., Sesack, S. R., and Michael, A. C. (2012) Domain-dependent effects of DAT inhibition in the rat dorsal striatum. *J. Neurochem.* 122, 283–294.
- (70) Garris, P. A., and Wightman, R. M. (1995) Distinct pharmacological regulation of evoked dopamine efflux in the amygdala and striatum of the rat in vivo. *Synapse* 20, 269–279.
- (71) Jones, S. R., Garris, P. A., and Wightman, R. M. (1995) Different effects of cocaine and nomifensine on dopamine uptake in the caudate-putamen and nucleus accumbens. *J. Pharmacol. Exp. Ther.* 274, 396–403.
- (72) Belle, A. M., Owesson-White, C., Herr, N. R., Carelli, R. M., and Wightman, R. M. (2013) Controlled Iontophoresis Coupled with Fast-Scan Cyclic Voltammetry/Electrophysiology in Awake, Freely Moving Animals. *ACS Chem. Neurosci.* 4, 761–771.
- (73) Wu, Q., Reith, M. E., Kuhar, M. J., Carroll, F. I., and Garris, P. A. (2001) Preferential increases in nucleus accumbens dopamine after systemic cocaine administration are caused by unique characteristics of dopamine neurotransmission. *J. Neurosci.* 21, 6338–6347.
- (74) Yang, H., and Michael, A. C. (2007) In Vivo Fast-Scan Cyclic Voltammetry of Dopamine near Microdialysis Probes. In *Electrochemical Methods for Neuroscience* (Michael, A. C., and Borland, L. M., Eds.), CRC Press, Boca Raton, FL.
- (75) Yang, H., Peters, J. L., and Michael, A. C. (1998) Coupled effects of mass transfer and uptake kinetics on in vivo microdialysis of dopamine. *J. Neurochem.* 71, 684–692.
- (76) Kita, J. M., Parker, L. E., Phillips, P. E., Garris, P. A., and Wightman, R. M. (2007) Paradoxical modulation of short-term

facilitation of dopamine release by dopamine autoreceptors. *J. Neurochem.* 102, 1115–1124.

(77) Ciliax, B. J., Heilman, C., Demchyshyn, L. L., Pristupa, Z. B., Ince, E., Hersch, S. M., Niznik, H. B., and Levey, A. I. (1995) The dopamine transporter: Immunohistochemical characterization and localization in brain. *J. Neurosci.* 15, 1714–1723.

(78) Freed, C., Revay, R., Vaughan, R. A., Kriek, E., Grant, S., Uhl, G. R., and Kuhar, M. J. (1995) Dopamine transporter immunoreactivity in rat brain. *J. Comp. Neurol.* 359, 340–349.

(79) Sesack, S. R., Hawrylak, V. A., Matus, C., Guido, M. A., and Levey, A. I. (1998) Dopamine axon varicosities in the prelimbic division of the rat prefrontal cortex exhibit sparse immunoreactivity for the dopamine transporter. *J. Neurosci.* 18, 2697–2708.

(80) Winslow, B. D., Christensen, M. B., Yang, W. K., Solzbacher, F., and Tresco, P. A. (2010) A comparison of the tissue response to chronically implanted Parylene-C-coated and uncoated planar silicon microelectrode arrays in rat cortex. *Biomaterials* 31, 9163–9172.

(81) Bezaud, E., Dovero, S., Imbert, C., Boraud, T., and Gross, C. E. (2000) Spontaneous long-term compensatory dopaminergic sprouting in MPTP-treated mice. *Synapse* 38, 363–368.

(82) Finkelstein, D. I., Stanic, D., Parish, C. L., Tomas, D., Dickson, K., and Horne, M. K. (2000) Axonal sprouting following lesions of the rat substantia nigra. *Neuroscience* 97, 99–112.

(83) Barlow, A. L., Macleod, A., Noppen, S., Sanderson, J., and Guerin, C. J. (2010) Colocalization analysis in fluorescence micrographs: verification of a more accurate calculation of Pearson's correlation coefficient. *Microsc. Microanal.* 16, 710–724.

(84) Dunn, K. W., Kamocka, M. M., and McDonald, J. H. (2011) A practical guide to evaluating colocalization in biological microscopy. *Am. J. Physiol.: Cell Physiol.* 300, C723–742.